Pharmaceutical Sciences and Drug Design
ISSN: 3062-4428
2024, Volume 4, Page No: 249-261

Available online at: www.galaxypub.co/page/journals

Galaxy Publication

Galaxy Publication

Aptamer- and Transferrin-Codecorated Nanoparticles for Synergistic Delivery of Daunorubicin and Luteolin in Leukemia

Anders Nilsson[1]*, Sofia Lindberg[2], Karin Holm[1]

[1]Department of Pharmaceutical Biosciences, Faculty of Pharmacy, Uppsala University, Uppsala, Sweden.
[2]Department of Drug Design, Faculty of Pharmacy, University of Gothenburg, Gothenburg, Sweden.

***E-mail** ✉ anders.nilsson@gmail.com

Received: 15 August 2024; **Revised:** 28 November 2024; **Accepted:** 29 November 2024

ABSTRACT

The purpose of this research was to create a binary nanodrug-delivery platform functionalized with aptamers (APs) and transferrin (Tf), and encapsulating daunorubicin (Drn) and luteolin (Lut) for leukemia therapy. Oligonucleotide ligands containing APs and Tf were designed and synthesized independently. AP-functionalized nanoparticles loaded with Drn (AP-Drn NPs) and Tf-functionalized nanoparticles loaded with Lut (Tf-Lut NPs) were fabricated through self-assembly. A binary nanodrug-delivery system co-functionalized with APs and Tf and co-loaded with Drn and Lut (AP/Tf-Drn/Lut NPs) was constructed via self-assembly of AP-Drn NPs and Tf-Lut NPs. The in vitro and in vivo performance of this system was assessed using a leukemia cell line and a tumor-bearing mouse model, compared to formulations decorated with a single ligand, loaded with a single drug, or free-drug combinations. The AP/Tf-Drn/Lut NPs were spherical with a nanoscale size (187.3 ± 5.3 nm) and exhibited drug-loading efficiency of approximately 85%. In vitro, the cytotoxicity of AP/Tf-Drn/Lut NPs was substantially greater than that of single-ligand-functionalized nanoparticles. The dual-drug-loaded AP/Tf-Drn/Lut NPs demonstrated superior inhibition of tumor cells compared to single-drug-loaded versions, indicating a synergistic effect between the two drugs. In vivo, AP/Tf-Drn/Lut NPs displayed the highest antileukemic efficacy with no observable toxicity. This study demonstrated that AP/Tf-Drn/Lut NPs represent a promising targeted drug-delivery platform for leukemia treatment, attributable to the synergistic action of the co-encapsulated drugs. Limitations of the system include stability challenges during scale-up production and translation from laboratory to clinical application.

Keywords: Acute myeloid leukemia, Daunorubicin, Luteolin, Aptamer, Transferrin, Nanodrug-delivery system

How to Cite This Article: Nilsson A, Lindberg S, Holm K. Aptamer- and Transferrin-Codecorated Nanoparticles for Synergistic Delivery of Daunorubicin and Luteolin in Leukemia. Pharm Sci Drug Des. 2024;4:249-61. https://doi.org/10.51847/XrjeAbbC1h

Introduction

Acute myeloid leukemia (AML), a heterogeneous blood cancer, represents the most frequent acute leukemia in adults [1]. Clinical prognosis for AML patients remains unfavorable, with 5-year survival rates below 30% and significantly higher incidence plus nearly 90% mortality in elderly patients (>65 years) [2, 3]. Standard treatments for AML primarily include conventional chemotherapy (typically cytarabine combined with daunorubicin [Drn] or idarubicin), targeted agents such as FLT3 inhibitors (e.g., midostaurin, quizartinib, and cabozantinib), and immunotherapies like gemtuzumab ozogamicin (an anti-CD33 antibody conjugated to calicheamicin) [3–6]. Despite these options, existing therapies face major challenges, including poor patient compliance due to severe toxicity and reduced effectiveness from drug resistance. Thus, there is an urgent need to develop novel therapeutic approaches to enhance outcomes.

In recent years, nanoparticle (NP)-based combination therapies have gained considerable interest for AML management. Two liposomal products are currently approved clinically for hematologic malignancies: liposomal Drn (DaunoXome) and liposomal cytarabine + Drn (CPX-351/VYXEOS) [7, 8]. Phase III trials showed that the liposomal co-formulation of Drn and cytarabine markedly improved median overall survival (9.56 vs 5.95 months)

and complete remission rates (47.7% vs 33.3%) compared to free drugs in elderly patients with newly diagnosed high-risk secondary AML [9]. This has ushered in a new phase of Drn-based nano-combination therapy for AML. Daunorubicin (Drn), an anthracycline topoisomerase inhibitor, is a widely used agent against hematologic malignancies, including AML, adult acute nonlymphocytic leukemia, and acute lymphocytic leukemia in both children and adults [10]. However, multidrug resistance has limited the broader clinical use of Drn injections. Recently, traditional Chinese herbal compounds and nanotechnology have emerged as promising strategies to circumvent multidrug resistance [11, 12]. Luteolin (Lut; 3′,4′,5,7-tetrahydroxyflavone), a flavonoid used in traditional Chinese medicine for various conditions such as inflammation, cardiovascular diseases, and cancer [13, 14], has shown potential to potentiate chemotherapeutic effects against leukemia and reverse multidrug resistance through mechanisms including P-gp and BCL2 upregulation, MCL1 downregulation, and apoptosis induction in HL60 cells via c-Jun activation and histone H3 acetylation-mediated Fas/FasL expression [15–18]. No prior reports were found on co-formulating Drn and Lut within a single nanoplatform for leukemia therapy. Accordingly, this study explored the combination of Drn and Lut to achieve enhanced cytotoxicity and reduced resistance.

Aptamers (APs) bind targets with high specificity and affinity, and AP-directed delivery systems hold substantial promise for AML treatment [19]. Oligonucleotide APs can selectively target biomarkers overexpressed on AML cells, such as CD117 [20]. Additionally, AML cells overexpress transferrin (Tf) receptors, enabling Tf-conjugated nanoparticles to deliver drugs specifically to tumor cells [21]. Polyethylene glycol (PEG) serves as a versatile linker for attaching ligands covalently; its terminal groups can be modified to amine, carboxylic acid, or sulfhydryl functionalities, allowing efficient conjugation via amide bonds or disulfide bridges [22]. In this work, PEG was employed as a linker to functionalize nanoparticles with both APs and Tf.

Here, we developed a binary nanodrug-delivery system co-functionalized with APs and Tf and co-loaded with Drn and Lut (AP/Tf-Drn/Lut NPs) for AML therapy. The in vitro and in vivo efficacy of this platform was investigated in a leukemia cell line and tumor-bearing mouse model, benchmarked against single-ligand-functionalized, single-drug-loaded, and free-drug formulations.

Materials and Methods

Materials

Daunorubicin (Drn), luteolin (Lut), oleic acid (OA), phosphatidylglycerol, iron-free human transferrin (Tf), and N-hydroxysuccinimide (NHS) were procured from Sigma (St Louis, MO, USA). In contrast, (2,3-dioleoyloxy-propyl)-trimethylammonium (DOTAP) was supplied by Avanti Polar Lipids (Birmingham, AL, USA). Both NH2-PEG-COOH and DSPE-PEG-COOH were acquired from Ponsure Biological (Shanghai, China). The HL60 human promyelocytic leukemia cell line was sourced from the American Type Culture Collection (Manassas, VA) and grown in Dulbecco's modified Eagle's medium (DMEM) with 10% fetal bovine serum (FBS) supplementation, under conditions of 37°C and 5% CO2.

Animals

Female BALB/c nude mice aged 4–6 weeks were supplied by Beijing Vital River Laboratory Animal Technology (Beijing, China). All procedures involving animals adhered to the National Institutes of Health Guide for the Care and Use of Laboratory Animals. Experimental protocols received approval from the Animal Ethics Committee at Qingdao Hospital of Traditional Chinese Medicine.

Synthesis of AP–polyethylene glycol–Oleic Acid

The synthesis began with preparation of PEG-OA. NH2-PEG-COOH along with triethylamine (TEA) was dissolved in dimethyl sulfoxide (DMSO), followed by addition to a DMSO solution containing OA, dicyclohexylcarbodiimide (DCC), and NHS. This mixture was stirred for 12 h at ambient temperature [20]. The resulting OA-PEG-COOH was recovered through filtration. Next, a CD117-targeting aptamer (AP) was linked to OA-PEG-COOH to generate AP-PEG-OA conjugates. For this, OA-PEG-COOH underwent NHS activation before reaction with a 5'-amino-functionalized CD117-specific oligonucleotide aptamer. The reactants were agitated overnight at room temperature, followed by purification via high-performance liquid chromatography (HPLC) and freeze-drying, yielding AP-PEG-OA as off-white solids. Conjugation success was validated using an enhanced BCA protein assay kit with absorbance measurement at 562 nm.

Synthesis of Tf-PEG-DSPE

Tf-PEG-DSPE was created via amide bond formation linking Tf to DSPE-PEG-COOH [21]. DSPE-PEG-COOH, DCC, and NHS were first dissolved in DMSO and stirred for 10 h. Tf and TEA were then introduced, and stirring continued for another 10 h under nitrogen protection at room temperature. The product was filtered, dialyzed, and lyophilized to isolate Tf-PEG-DSPE. Structural confirmation was achieved through infrared spectroscopy and 1H NMR analysis.

Preparation of nanodrug-delivery system

Nanoparticles loaded with Drn and decorated with AP (AP-Drn NPs) **(Figure 1a)**, as well as those loaded with Lut and decorated with Tf (Tf-Lut NPs) **(Figure 1a)**, were fabricated employing the thin-film hydration technique [23]. To prepare AP-Drn NPs, AP-PEG-OA (200 mg) and Drn (100 mg) were dissolved in 5 mL acetone. Solvent was evaporated under reduced pressure in a 60°C water bath to deposit a thin film. This film was then hydrated with deionized water containing 0.5% (w/v) DOTAP to form the nanoparticles. Similarly, for Tf-Lut NPs, Tf-PEG-DSPE (200 mg), Lut (100 mg), and phosphatidylglycerol (20 mg) were dissolved in 5 mL acetone, followed by solvent removal under reduced pressure at 60°C to create a thin film. Hydration was performed with deionized water to obtain the nanoparticles.

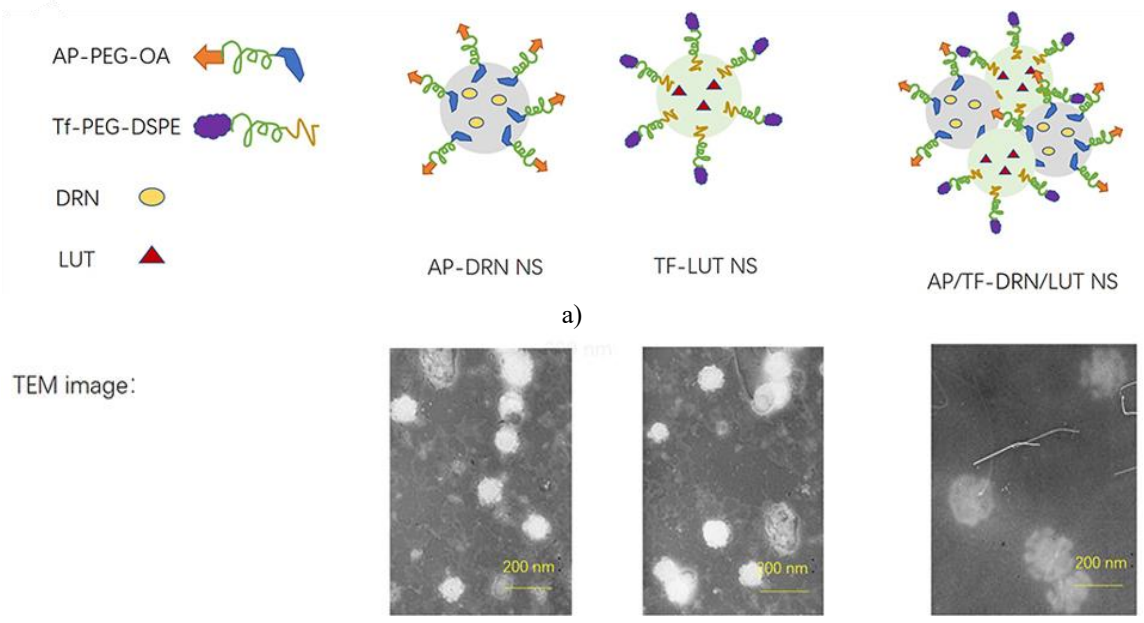

Figure 1 Scheme (a) and TEM images (b) of AP/Tf-Drn/Lut NPs.

Note: AP/Tf-Drn/Lut NPs were nanosized with some ligands on the spherical surface.

The co-decorated, co-loaded nanoparticles (AP/Tf-Drn/Lut NPs) **(Figure 1a)** were formed through self-assembly process [22]. AP-Drn NPs were combined with Tf-Lut NPs while stirring at 400 rpm. A ligand-only control without drugs (AP/Tf NPs) was made similarly but omitting the therapeutic agents. Mono-ligand versions co-loaded with both drugs (AP-Drn/Lut NPs or Tf-Drn/Lut NPs) were generated by replacing AP-PEG-OA with PEG-OA or Tf-PEG-DSPE with PEG-DSPE, accordingly. All prepared nanoparticle suspensions were freeze-dried and kept at 4°C for storage.

Characterization of nanodrug-delivery system

Morphological features of AP-Drn NPs, Tf-Lut NPs, and AP/Tf-Drn/Lut NPs were assessed using transmission electron microscopy (JEOL, Tokyo, Japan) following negative staining with 3% sodium phosphotungstate solution [24]. Hydrodynamic diameter was determined via dynamic light scattering on a Beckman Coulter Delsa Nano C instrument (Fullerton, CA), while surface charge (ζ-potential) was measured with a Malvern Zetasizer (Malvern, UK). Drug encapsulation efficiency (EE) and loading capacity (LC) for both Drn and Lut were quantified by HPLC on a C18 column (150×4.6 mm, 12 nm pore size). The mobile phase consisted of 0.01 M

KH2PO4–acetonitrile–acetic acid (45:55:0.27 v:v:v) at a flow rate of 0.5 mL/min, with detection at 350 nm for Lut and 490 nm for Drn [25, 26].

Stability of nanodrug-delivery system

To assess stability, AP-Drn NPs, Tf-Lut NPs, and AP/Tf-Drn/Lut NPs were dispersed (20 mg in 10 mL) in phosphate-buffered saline (PBS) or cell culture medium (DMEM plus 10% FBS) at pH 7.4 and maintained at 37°C over 4 days [27]. Variations in particle diameter and encapsulation efficiency were tracked employing the characterization techniques outlined previously.

In vitro release assays

Drug release behavior from the various nanoparticle formulations was studied in vitro using dialysis tubing with a 3500 Da molecular weight cutoff [28]. Separate dialysis bags were loaded with 1 mL each of AP/Tf-Drn/Lut NPs, AP-Drn/Lut NPs, Tf-Drn/Lut NPs, AP-Drn NPs, or Tf-Lut NPs and submerged in 20 mL of PBS supplemented with 0.5% Tween 80. The system was kept at 37°C with gentle agitation (100 rpm). At selected time intervals, 200 μL of the external medium was sampled, immediately replaced with the same volume of fresh buffer, and the released amounts of Drn and Lut were measured by HPLC.

Cellular uptake

To investigate nanoparticle internalization by cells, coumarin 6 was co-incorporated as a fluorescent probe during nanoparticle preparation, as detailed in the "Preparation of nanodrug-delivery system" section [29]. HL60 cells were plated in 24-well formats at a density of 105 cells per well. The different nanoparticle systems were introduced, and incubation proceeded for either 1 h or 24 h. Afterward, cells underwent triple washing with D-Hank's solution, were detached and pelleted by centrifugation, and fluorescence intensity reflecting uptake was analyzed via BD FACSCalibur flow cytometry.

Cytotoxicity assays

Cytotoxic potential of AP/Tf-Drn/Lut NPs and the control formulations was assessed through MTS reduction assays [30]. HL60 cells were first seeded into 96-well plates and incubated overnight to allow attachment, followed by medium exchange. Cells were then treated for 48 h with AP/Tf-Drn/Lut NPs, AP-Drn/Lut NPs, Tf-Drn/Lut NPs, AP-Drn NPs, Tf-Lut NPs, free Drn/Lut mixture, free Drn alone, or free Lut alone. Subsequently, 15 μL of MTS reagent was introduced per well, and plates were returned to 37°C for another 4 h. Absorbance values were recorded at 490 nm on a plate reader, and viability percentages were computed relative to untreated controls.

Drug combination

Potential synergism between Drn and Lut was determined by combination index (CI) analysis based on the Chou–Talalay approach [31]. The CI value corresponding to 50% growth inhibition (CI50) was calculated as CI50 = (D)Drn/(D50)Drn + (D)Lut/(D50)Lut, wherein (D)Drn and (D)Lut are the respective drug concentrations in the dual-loaded AP/Tf-Drn/Lut NPs that achieved 50% cell kill, while (D50)Drn and (D50)Lut are the concentrations needed for the same effect using the corresponding mono-drug nanoparticles (AP-Drn NPs or Tf-Lut NPs). CI50 values below 1 denote synergy, equal to 1 indicate an additive effect, and above 1 suggest antagonism.

In vivo AML-therapy efficiency

An HL60-derived leukemia xenograft was generated in BALB/c nude mice by injecting 106 cells suspended in 150 μL PBS subcutaneously into the left flank. Tumor dimensions were tracked with calipers, and volume estimated by the formula $L \times W^2/2$ (L = longest diameter, W = perpendicular width) [32]. When tumors averaged ~100 mm^3, animals were randomized into ten groups (n=8 each) and received tail-vein injections on days 0, 3, 6, 9, 12, 15, 18, and 21 of: AP/Tf-Drn/Lut NPs (Drn 5 mg/kg + Lut 2 mg/kg), AP-Drn/Lut NPs (Drn 5 mg/kg + Lut 2 mg/kg), Tf-Drn/Lut NPs (Drn 5 mg/kg + Lut 2 mg/kg), AP-Drn NPs (Drn 10 mg/kg), Tf-Lut NPs (Lut 4 mg/kg), drug-free AP/Tf NPs, free Drn/Lut (Drn 5 mg/kg + Lut 2 mg/kg), free Drn (10 mg/kg), free Lut (4 mg/kg), or normal saline (0.9%). Animal body weights were recorded across the 21-day treatment window. Additionally, serum markers—creatinine (Cre, for kidney status), alanine aminotransferase (ALT, for liver status), and white blood cell counts (WBC)—were examined.

In vivo pharmacokinetics and biodistribution

For pharmacokinetic and tissue distribution studies, mice were divided randomly into four groups (n=8) and given single intravenous doses of AP/Tf-Drn/Lut NPs, AP-Drn/Lut NPs, Tf-Drn/Lut NPs, or free Drn/Lut (dosed at Drn 5 mg/kg and/or Lut 2 mg/kg) [33]. Heparinized blood was sampled at preset intervals, plasma isolated via centrifugation (1000 g, 10 min), deproteinized with three volumes of methanol, and clarified by further centrifugation (1000 g, 5 min). At 1 h and 48 h after dosing, organs (heart, liver, lung, kidney, spleen), bone marrow, and tumors were collected and homogenized in saline. Bone marrow samples were obtained by flushing femurs and tibias with RPMI medium (Gibco) containing 5% FBS using a 28-gauge needle [34]. Drug extraction from homogenates employed hexane–diethyl ether (3:1 v/v), followed by centrifugation (1000 g, 10 min) and recovery of the organic layer. Quantitation of Drn and Lut in plasma and tissues followed the HPLC protocol described earlier in the "Characterization of nanodrug-delivery system" section.

Statistical analysis

All data are reported as mean ± standard deviation (SD). Intergroup comparisons employed unpaired Student's t-tests for pairwise analyses or one-way ANOVA for multiple groups, performed in SPSS 19.0. Differences achieving $P<0.05$ were considered statistically significant.

Results and Discussion

Characterization of AP-PEG-OA and Tf-PEG-DSPE

To verify the successful attachment of AP to PEG-OA, the absorbance of eluates from AP-PEG-OA and unbound AP was assessed individually at 562 nm via an enhanced BCA protein assay kit. Unbound AP showed a single peak in the 12–15 min range, whereas AP-PEG-OA revealed two distinct peaks—one aligning with the unbound AP peak—confirming effective conjugation. The successful preparation of Tf-PEG-DSPE was validated through infrared (IR) spectroscopy and ^{1}H NMR analysis. IR peaks: 3621.3 (–NH–, –OH), 1898.5 (–C=O), 1665.1 (–HN–CO–), 1621.7 (–HN–CO–). ^{1}H NMR ($CDCl_3$, 300 MHz) δ (ppm): 0.89 (–CH_3), 1.12–1.97 (DSPE protons), 2.33 (–$COCH_2$–), 2.42 (–$COCH_2CH_2$–), 2.61 (–CH_2N–), 3.39 (–OCH_3–), 3.70–4.10 (PEG protons), 5.82 (–NH–). Synthesis yields were 73.9% for AP-PEG-OA and 78.6% for Tf-PEG-DSPE.

Characterization of nanodrug-delivery system

The nanoparticles AP/Tf-Drn/Lut NPs, AP-Drn NPs, and Tf-Lut NPs displayed spherical shapes **(Figure 1b).** AP/Tf-Drn/Lut NPs had an average diameter of 187.3 ± 5.3 nm **(Table 1)**, exceeding the sizes of AP-Drn NPs (91.5 ± 2.8 nm) and Tf-Lut NPs (88.7 ± 2.5 nm). With the exception of positively charged AP-Drn NPs (18.9 ± 1.7 mV), the remaining formulations possessed negative zeta potentials. Encapsulation efficiency (EE) surpassed 85% across AP/Tf-Drn/Lut NPs and the comparative systems. Over a 4-day observation period, particle size and EE remained largely unchanged for AP/Tf-Drn/Lut NPs, AP-Drn NPs, and Tf-Lut NPs **(Figures 2a and 2b)**, in agreement with observations by Chen *et al*. [35] and supporting the robustness of these nanoparticles.

Table 1. Characterization of nanodrug-delivery systems (means ± SD, n=3)

Formulation	Particle Size (nm)	Polydispersity Index (PDI)	Zeta Potential (mV)	Donepezil Encapsulation Efficiency (%)	Donepezil Loading Capacity (%)	Luteolin Encapsulation Efficiency (%)	Luteolin Loading Capacity (%)
AP/Tf-Donepezil/Luteolin Nanoparticles	187.3 ± 5.3	0.142 ± 0.019	−25.4 ± 2.6	88.7 ± 3.9	5.2 ± 0.5	85.9 ± 4.2	2.1 ± 0.4
AP-Donepezil/Luteolin Nanoparticles	186.7 ± 4.7	0.139 ± 0.023	−19.2 ± 2.1	87.5 ± 3.8	5.9 ± 0.6	86.7 ± 3.7	2.4 ± 0.6
Tf-Donepezil/Luteolin Nanoparticles	188.3 ± 4.5	0.126 ± 0.016	−17.5 ± 1.8	86.5 ± 4.1	5.7 ± 0.6	88.3 ± 3.9	2.2 ± 0.5
AP-Donepezil Nanoparticles	91.5 ± 2.8	0.112 ± 0.011	+18.9 ± 1.7	89.4 ± 4.4	11.8 ± 1.1	-	-
Tf-Luteolin Nanoparticles	88.7 ± 2.5	0.128 ± 0.014	−38.9 ± 3.1	-	-	86.5 ± 3.6	4.6 ± 0.7

AP/Tf Nanoparticles	187.8 ± 5.1	0.147 ± 0.026	−37.6 ± 2.9	-	-	-	-

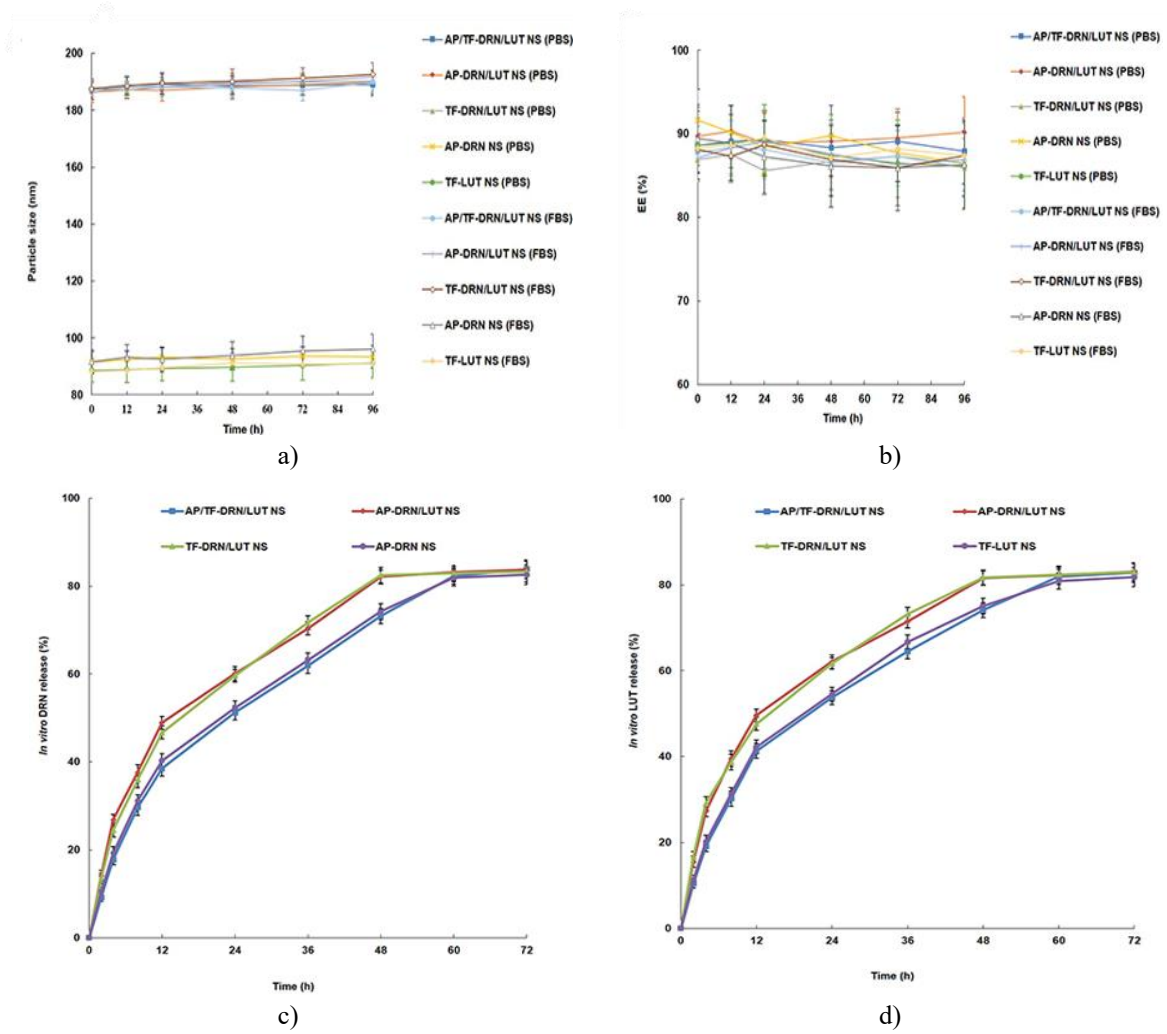

Figure 2. Changes in particle size (a) and EE (b) analyzed in PBS and culture medium (FBS). In vitro drug-release behavior of Drn (c) or Lut (d) from nanosystems evaluated by dialysis.

Notes: Sustained drug-release patterns were found for all the samples tested. Data presented as means ± SD, n=3.

Table 2. Cellular uptake percentages (means ± SD, n=8)

Formulations	1 h	24 h
AP/Tf-Drn/Lut NPs	73.1±3.6	65.8±3.3
AP-Drn/Lut NPs	59.5±3.2	55.6±2.8
Tf-Drn/Lut NPs	57.1±2.9	54.2±3.1
AP-Drn NPs	60.2±3.3	53.1±2.6
Tf-Lut NPs	58.4±2.7	52.5±2.8
AP/Tf NPs	74.3±3.5	64.7±3.2

In vitro release assays

Every formulation examined exhibited prolonged release profiles **(Figures 2c and 2d).** The dual-ligand AP/Tf-Drn/Lut NPs released drugs more gradually than their single-ligand counterparts. Considering Drn release specifically **(Figure 2c),** full release from AP/Tf-Drn/Lut NPs and AP-Drn NPs required 60 h, in contrast to 48 h for AP-Drn/Lut NPs and Tf-Drn/Lut NPs.

Cellular uptake

Uptake results for the various nanoparticles are detailed in **Table 2**. High uptake rates were observed across all systems at 1 h and 24 h time points. Nanoparticles modified with both ligands (AP/Tf-Drn/Lut NPs and AP/Tf NPs) achieved significantly superior uptake compared to those with a single ligand ($P < 0.05$), suggesting enhanced targeting from the ligand combination. This outcome corresponds with prior work by Jing *et al*. [36].

Cytotoxicity and drug combinations

AP/Tf-Drn/Lut NPs demonstrated markedly superior cytotoxicity relative to single-ligand versions AP-Drn/Lut NPs and Tf-Drn/Lut NPs ($P < 0.05$), **(Figure 3)**. Each of the single-ligand dual-drug systems outperformed the free Drn/Lut combination in cytotoxicity ($P < 0.05$). Dual-drug AP/Tf-Drn/Lut NPs provided stronger suppression of tumor cell growth than single-drug AP-Drn NPs or Tf-Lut NPs ($P < 0.05$), likely resulting from drug synergy. Combination index (CI_{50}) calculations, presented in **Table 3**, substantiated this, with the 5:2 Drn:Lut ratio yielding the minimal CI_{50} of 0.792 and thus optimal synergy. This 5:2 (w:w) ratio was therefore adopted for nanoparticle fabrication.

Table 3. CI_{50} values of AP/Tf-Drn/Lut NPs when different Drn:Lut weight ratios were applied (means ± SD, n=8)

Formulation	Donepezil:Luteolin Ratio (w:w)	IC_{50} of Donepezil (μM)	IC_{50} of Luteolin (μM)	Combination Index (CI_{50})
AP-Donepezil Nanoparticles	-	0.93 ± 0.09	-	-
Tf-Luteolin Nanoparticles	-	-	1.16 ± 0.12	-
AP/Tf-Donepezil/Luteolin Nanoparticles	5:1	0.79 ± 0.08	1.06 ± 0.11	0.987
AP/Tf-Donepezil/Luteolin Nanoparticles	5:2	0.56 ± 0.05	0.22 ± 0.03	0.792
AP/Tf-Donepezil/Luteolin Nanoparticles	1:1	0.45 ± 0.04	0.45 ± 0.04	0.872
AP/Tf-Donepezil/Luteolin Nanoparticles	2:5	0.29 ± 0.03	0.73 ± 0.09	0.941
AP/Tf-Donepezil/Luteolin Nanoparticles	1:5	0.18 ± 0.02	0.90 ± 0.10	0.969

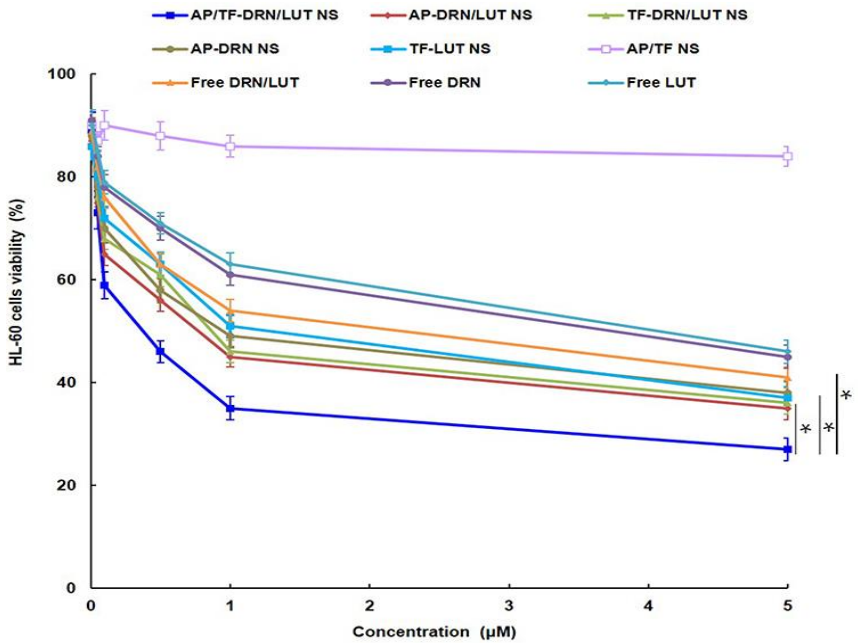

Figure 3. Cytotoxicity of AP/Tf-Drn/Lut NPs and other formulations evaluated with MTS assays.

Notes: Cytotoxicity of AP/Tf-Drn/Lut NPs was remarkably higher than single ligand–decorated NPs, single drug–loaded NPs, and free drugs. Data presented as means ± SD, n=6. *$P < 0.05$.

In vivo AML-therapy efficiency

All formulations containing drugs substantially impeded tumor progression versus the saline control ($P < 0.05$), **(Figure 4a).** Among them, AP/Tf-Drn/Lut NPs delivered the greatest therapeutic impact on AML, outperforming single-ligand, single-drug, and free-drug counterparts ($P < 0.05$). Nanoparticle-delivered drugs consistently

showed better efficacy than free-drug administrations ($P < 0.05$). Body weights of mice receiving drug-loaded nanoparticles stayed stable, unlike the declines seen in saline and blank nanoparticle groups ($P < 0.05$**), (Figure 4b).** Nanoparticle treatments induced only minor variations in ALT, Cre, and WBC counts relative to controls.

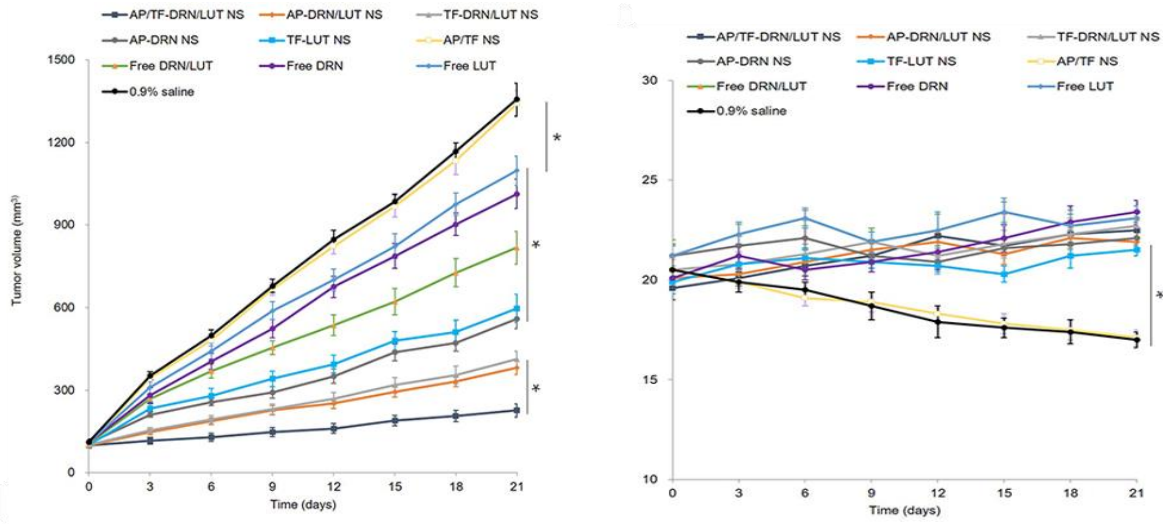

a) b)

Figure 4. In vivo AML therapy efficiency: Tumor size (a) and body weight (b).

Notes: AP/Tf-Drn/Lut NPs exhibited the most remarkable AML therapy efficiency compared with single ligand–decorated, single drug–loaded and free-drug groups. Data presented as means ± SD, n=8. *P < 0.05.

In vivo pharmacokinetics and biodistribution

Key pharmacokinetic metrics—such as area under the concentration-time curve (AUC), maximum plasma concentration (Cmax), and elimination half-life (t½)—are detailed in **Tables 4 and 5**. For Lut, as a representative case, AP/Tf-Drn/Lut NPs achieved a higher AUC (431.25 ± 11.38 mg/L/h) than AP-Drn/Lut NPs (311.26 ± 8.34 mg/L/h), Tf-Drn/Lut NPs (289.86 ± 7.65 mg/L/h), or free Drn/Lut (198.63 ± 4.59 mg/L/h; $P < 0.05$). Regarding Drn, AP/Tf-Drn/Lut NPs displayed elevated Cmax (55.36 ± 3.21 L/kg/h) and prolonged t½ (12.37 ± 0.78 h) relative to the remaining formulations. Drug levels across tumor and organ tissues are illustrated in **Figure 5**. At 1 h and 48 h following injection, AP/Tf-Drn/Lut NPs demonstrated superior tumor targeting over the single-ligand AP-Drn/Lut NPs and Tf-Drn/Lut NPs ($P < 0.05$), while both nanoparticle versions accumulated more in tumors than free Drn/Lut ($P < 0.05$). In contrast, at 1 h, free Drn/Lut showed increased renal uptake compared to the loaded nanoparticles ($P < 0.05$).

Table 4. Pharmacokinetic parameters for Drn (means ± SD, n=8)

Pharmacokinetic Parameter	Unit	AP/Tf-Donepezil/Luteolin Nanoparticles	AP-Donepezil/Luteolin Nanoparticles	Tf-Donepezil/Luteolin Nanoparticles	Free Donepezil/Luteolin
C_{max} (Maximum concentration)	μg/L/h	55.36 ± 3.21*	42.31 ± 2.98*	40.55 ± 2.74*	29.83 ± 2.88
t½ (Elimination half-life)	h	12.37 ± 0.78*	9.72 ± 0.64*	8.84 ± 0.53*	1.89 ± 0.31
AUC_{0-t} (Area under the curve from 0 to t)	mg/L·h	659.72 ± 19.56*	512.33 ± 17.14*	488.75 ± 21.16*	256.81 ± 9.18
$AUC_{0-\infty}$ (Area under the curve from 0 to infinity)	mg/L·h	662.31 ± 20.05*	519.64 ± 19.47*	493.23 ± 22.44*	404.73 ± 9.26

Note: *P < 0.05 compared with free Drn/Lut.

Abbreviations: Cmax, plasma drug peak concentration; t½, half-life; AUC_{0-t}, area under curve of time 0 to last time point; $AUC_{0-\infty}$, area under curve of time 0 to maximum.

Table 5. Pharmacokinetic parameters for Lut (mean ± SD, n=8)

Pharmacokinetic Parameter	Unit	AP/Tf-Donepezil/Luteolin Nanoparticles	AP-Donepezil/Luteolin Nanoparticles	Tf-Donepezil/Luteolin Nanoparticles	Free Donepezil/Luteolin
C_{max} (Maximum concentration)	μg/L/h	35.47 ± 3.18*	28.11 ± 2.36*	26.59 ± 2.95*	18.31 ± 2.12
t½ (Elimination half-life)	h	8.98 ± 0.58*	5.46 ± 0.41*	5.31 ± 0.34*	1.51 ± 0.29
$AUC_{0–t}$ (Area under the curve from 0 to t)	mg/L·h	431.25 ± 11.38*	311.26 ± 8.34*	289.86 ± 7.65*	198.63 ± 4.59
$AUC_{0–\infty}$ (Area under the curve from 0 to infinity)	mg/L·h	439.35 ± 12.24*	317.64 ± 11.35*	295.61 ± 6.96*	202.34 ± 5.13

Note: *P < 0.05 compared with free Drn/Lut.

Abbreviations: Cmax, peak plasma drug concentration; t½, half-life; $AUC_{0–t}$, area under curve of time 0 to last time point; $AUC_{0–\infty}$, area under curve of time 0 to maximum.

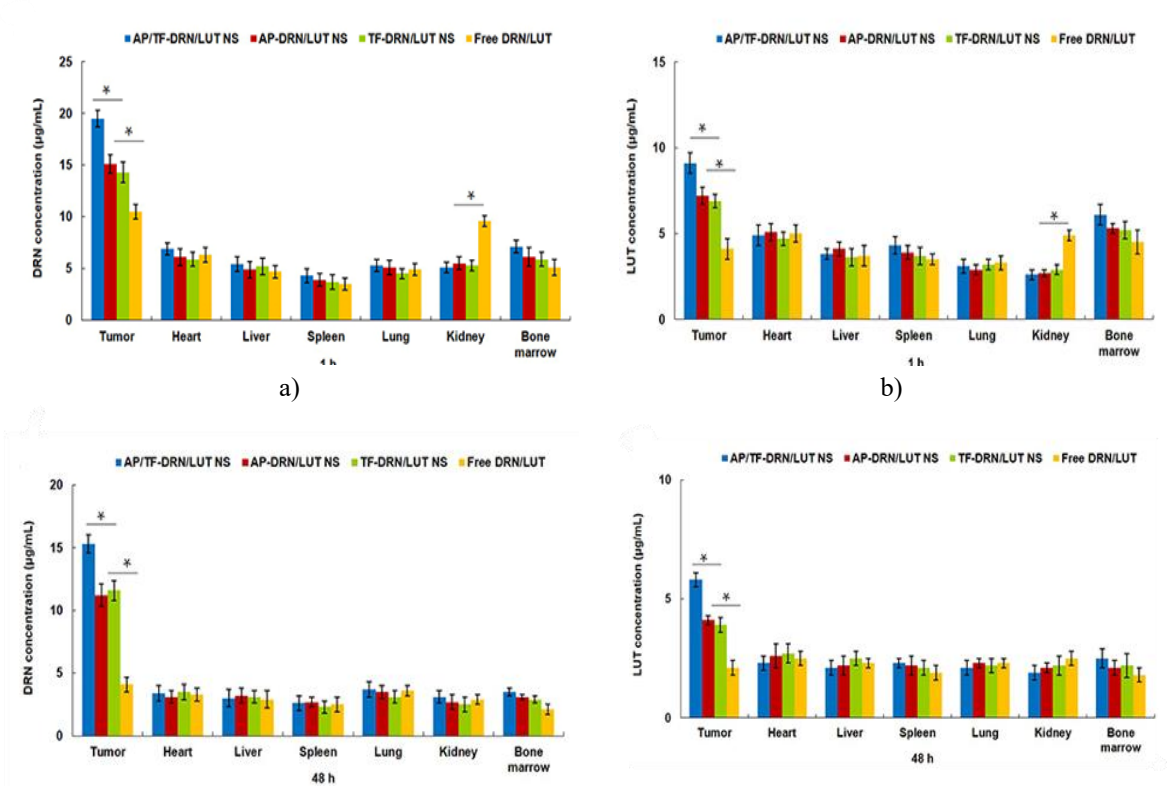

Figure 5. In vivo Drn (a and c) and Lut (b and d) distribution in tissue after 1 h (a and b) and 48 h (c and d) of drug administration. *P < 0.05.

Notes: AP/Tf-Drn/Lut NPs showed higher tumor-tissue distribution than single ligand–decorated AP-Drn/Lut NPs, Tf-Drn/Lut NPs, and free Drn/Lut. Data presented as means ± SD, n=8. *P < 0.05.

This investigation focused on engineering a nanoparticle platform co-functionalized with AP and Tf ligands and co-loaded with Drn and Lut to improve AML management. The process began with the creation of AP- and Tf-bearing conjugates. Separate production of positively charged AP-Drn NPs and negatively charged Tf-Lut NPs preceded their combination into AP/Tf-Drn/Lut NPs via charge-driven self-assembly. According to Choueiri *et al*. [37], adjustments in solvent makeup or ligand electrooxidation can fine-tune polymer-solvent affinities, extending the variety of ligands suitable for nanoparticle construction and opening avenues for innovative assembly strategies. Yang *et al*. [38] designed chitosan-based nanoparticles responsive to pH and glutathione through a combined self-assembly and cross-linking approach, addressing drawbacks of earlier techniques like limited stability, reduced drug loading, and constrained release mechanisms. Dong *et al*. [39] produced dual-peptide-targeted nanoparticles incorporating hyaluronic acid and EGFR ligands for delivering docetaxel and formononetin in prostate cancer models. The present effort adapted similar principles to formulate AP/Tf-Drn/Lut NPs tailored for leukemia.

AP/Tf-Drn/Lut NPs averaged 187 nm in diameter. Zhang *et al*. [40] noted that sub-200 nm particles exploit the enhanced permeability and retention phenomenon to boost tumor deposition, enabling lower doses and decreased adverse effects. Controlled release in vitro is essential for optimizing therapeutic impact. Pang *et al*. [41] constructed hyaluronic acid-functionalized carriers for simultaneous erlotinib and bevacizumab transport, reporting aligned release patterns for the paired agents—mirroring patterns seen here. Dual-ligand nanoparticles released payload more deliberately than single-ligand variants, possibly because greater ligand coverage on the surface restricts diffusion. Such surface modifications can indeed slow egress through physical obstruction, as observed by Dong *et al*. [39] Failure to attain full 100% release likely arises from drug sequestration inside the nanoparticle core.

Cell-based assays revealed markedly stronger cytotoxic effects from AP/Tf-Drn/Lut NPs versus single-ligand dual-drug nanoparticles, stemming from improved receptor-mediated uptake that increases internal drug concentrations and amplifies antitumor activity [42]. Dual-drug encapsulation in AP/Tf-Drn/Lut NPs also yielded greater growth inhibition than single-agent-loaded versions, presumably from complementary actions of Drn and Lut. Li *et al*. [43] highlighted the need to quantify synergy in multi-drug regimens, identifying combination index evaluation as a dependable tool. Employing the Chou–Talalay approach, [44] interactions were categorized as synergistic, additive, or opposing. A 5:2 Drn:Lut proportion produced the minimal CI_{50} (0.46), signifying maximal synergy, and guided the final nanoparticle composition.

In vivo pharmacokinetic and biodistribution experiments revealed that AP/Tf-Drn/Lut NPs exhibited elevated AUC, Cmax, t½, and greater drug accumulation in tumor tissue. Additionally, the nanosystems demonstrated prolonged circulation in the bloodstream, consistent with observations reported by Wang *et al*. [45] According to Jedrzejczyk *et al*. [46], Tf-based conjugates can serve as effective carriers to elevate drug levels in leukemia cells that overexpress Tf receptors, aligning with the enhanced tumor uptake seen here. The substantial increase in tumor deposition from drug-loaded nanoparticles relative to free-drug administrations can be attributed to the characteristic leaky vasculature of solid tumors, enabling passive targeting of nanosized carriers via the enhanced permeability and retention effect [47]. Li *et al*. [48] further noted that reduced renal drug distribution minimizes adverse effects and improves overall antitumor outcomes, an advantage realized by the nanoparticle formulations in this work.

Zhu *et al*. [49] reported that nanoparticle platforms can mitigate the toxicities associated with traditional chemotherapy while delivering superior in vivo anticancer performance. In their study, Tf-modified nanoparticles enhanced the AML-suppressive action of therapeutics in murine models. He *et al*. [50] established that APs bind to specific membrane receptors, facilitating cellular entry of attached nanoparticles and positioning them as valuable targeting moieties for AP-directed cancer drug delivery. The current investigation demonstrated that AP/Tf-Drn/Lut NPs provided the superior therapeutic efficacy against AML compared to single-ligand-modified, single-drug-loaded, or free-drug counterparts, precisely fulfilling the study's objective of harnessing combined dual ligands and dual drugs. Mouse body weights remained stable following administration of drug-loaded formulations, whereas the saline control group experienced weight decline. Wang *et al*. [51] attributed such weight loss during therapy to decreased appetite, lethargy, and reduced activity. In this research, AP/Tf-Drn/Lut NPs accomplished potent antitumor activity—nearly fully halting tumor progression—while avoiding weight-loss-associated toxicity, in agreement with results from Liu *et al*. [52]

Conclusion

Overall, AP/Tf-Drn/Lut NPs displayed substantially greater cytotoxicity compared to their single-ligand counterparts. Dual-drug-loaded AP/Tf-Drn/Lut NPs achieved stronger suppression of tumor cells than single-drug-loaded nanoparticles, confirming the synergistic interaction between the two agents. In vivo, AP/Tf-Drn/Lut NPs delivered the highest antileukemic efficacy with no evident toxicity, positioning them as a potential advanced delivery platform for targeted leukemia therapy through the combined synergy of the incorporated drugs. Potential drawbacks of this platform involve maintaining stability during scale-up manufacturing and translating from laboratory to clinical use.

Acknowledgments: None

Conflict of Interest: None

Financial Support: None

Ethics Statement: None

References

1. Estey E, Döhner H. Acute myeloid leukaemia. *Lancet*. 2006;368(9550):1894–1907. doi:10.1016/S0140-6736(06)69780-8
2. Daver N, Schlenk RF, Russell NH, Levis MJ. Targeting FLT3 mutations in AML: review of current knowledge and evidence. *Leukemia*. 2019;33(2):299–312. doi:10.1038/s41375-018-0357-9
3. Huang X, Lin H, Huang F, et al. Targeting approaches of nanomedicines in acute myeloid leukemia. *Dose Response*. 2019;17(4):1559325819887048. doi:10.1177/1559325819887048
4. Ferrara F, Vitagliano O. Induction therapy in acute myeloid leukemia: is it time to put aside standard 3 + 7? *Hematol Oncol*. 2019;37(5):558–563. doi:10.1002/hon.2615
5. Lin M, Chen B. Advances in the drug therapies of acute myeloid leukemia (except acute wpromyelocytic leukemia). *Drug Des Devel Ther*. 2018;12:1009–1017. doi:10.2147/DDDT.S161199
6. Norsworthy KJ, Ko CW, Lee JE, et al. Mylotarg for treatment of patients with relapsed or refractory CD33-positive acute myeloid leukemia. *Oncologist*. 2018;23(9):1103–1108. doi:10.1634/theoncologist.2017-0604
7. Latagliata R, Breccia M, Fazi P, et al. Liposomal daunorubicin versus standard daunorubicin: long term follow-up of the GIMEMA GSI 103 AMLE randomized trial in patients older than 60 years with acute myelogenous leukaemia. *Br J Haematol*. 2008;143(5):681–689. doi:10.1111/j.1365-2141.2008.07400.x
8. Maakaron JE, Mims AS. Daunorubicin-cytarabine liposome (CPX-351) in the management of newly diagnosed secondary AML: a new twist on an old cocktail. *Best Pract Res Clin Haematol*. 2019;32(2):127–133. doi:10.1016/j.beha.2019.05.005
9. Lancet JE, Uy GL, Cortes JE, et al. CPX-351 (cytarabine and daunorubicin) liposome for injection versus conventional cytarabine plus daunorubicin in older patients with newly diagnosed secondary acute myeloid leukemia. *J Clin Oncol*. 2018;36(26):2684–2692. doi:10.1200/JCO.2017.77.6112
10. Kaspers GJ, Zimmermann M, Reinhardt D, et al. Improved outcome in pediatric relapsed acute myeloid leukemia: results of a randomized trial on liposomal daunorubicin by the international BFM study group. *J Clin Oncol*. 2013;31(5):599–607. doi:10.1200/JCO.2012.43.7384
11. Jin J, Wang FP, Wei H, Liu G. Reversal of multidrug resistance of cancer through inhibition of P-glycoprotein by 5-bromotetrandrine. *Cancer Chemother Pharmacol*. 2005;55(2):179–188. doi:10.1007/s00280-004-0868-0
12. Hu CM, Zhang L. Nanoparticle-based combination therapy toward overcoming drug resistance in cancer. *Biochem Pharmacol*. 2012;83(8):1104–1111. doi:10.1016/j.bcp.2012.01.008
13. Kim YS, Kim SH, Shin J, et al. Luteolin suppresses cancer cell proliferation by targeting vaccinia-related kinase 1. *PLoS One*. 2014;9(10):e109655. doi:10.1371/journal.pone.0109655
14. Chian S, Li YY, Wang XJ, Tang XW. Luteolin sensitizes two oxaliplatin-resistant colorectal cancer cell lines to chemotherapeutic drugs via inhibition of the Nrf2 pathway. *Asian Pac J Cancer Prev*. 2014;15(6):2911–2916. doi:10.7314/APJCP.2014.15.6.2911
15. Zheng CH, Zhang M, Chen H, et al. Luteolin from flos chrysanthemi and its derivatives: new small molecule Bcl-2 protein inhibitors. *Bioorg Med Chem Lett*. 2014;24(19):4672–4677. doi:10.1016/j.bmcl.2014.08.034
16. Danışman Kalındemirtaş F, Birman H, Candöken E, Bilgiş Gazioğlu S, Melikoğlu G, Kuruca S. Cytotoxic effects of some flavonoids and imatinib on the K562 chronic myeloid leukemia cell line: data analysis using the combination index method. *Balkan Med J*. 2019;36(2):96–105. doi:10.4274/balkanmedj.galenos.2018.2017.1244
17. Chen PY, Tien HJ, Chen SF, et al. Response of myeloid leukemia cells to luteolin is modulated by differentially expressed Pituitary Tumor-Transforming Gene 1 (PTTG1) oncoprotein. *Int J Mol Sci*. 2018;19(4):1173. doi:10.3390/ijms19041173
18. Polier G, Giaisi M, Köhler R, et al. Targeting CDK9 by wogonin and related natural flavones potentiates the anti-cancer efficacy of the Bcl-2 family inhibitor ABT-263. *Int J Cancer*. 2015;136(3):688–698. doi:10.1002/ijc.29009

19. Wang M, Wu H, Duan M, et al. SS30, a novel thioaptamer targeting CD123, inhibits the growth of acute myeloid leukemia cells. *Life Sci*. 2019;232:116663. doi:10.1016/j.lfs.2019.116663
20. Zhao N, Pei SN, Qi J, et al. Oligonucleotide aptamer-drug conjugates for targeted therapy of acute myeloid leukemia. *Biomaterials*. 2015;67:42–51. doi:10.1016/j.biomaterials.2015.07.025
21. Kim TH, Jo YG, Jiang HH, et al. PEG-transferrin conjugated TRAIL (TNF-related apoptosis-inducing ligand) for therapeutic tumor targeting. *J Control Release*. 2012;162(2):422–428. doi:10.1016/j.jconrel.2012.07.021
22. van Vlerken LE, Vyas TK, Amiji MM. Poly (ethylene glycol)-modified nanocarriers for tumor-targeted and intracellular delivery. *Pharm Res*. 2007;24(8):1405–1414. doi:10.1007/s11095-007-9284-6
23. Nguyen CT, Tran TH, Amiji M, Lu X, Kasi RM. Redox-sensitive nanoparticles from amphiphilic cholesterol-based block copolymers for enhanced tumor intracellular release of doxorubicin. *Nanomedicine*. 2015;11(8):2071–2082. doi:10.1016/j.nano.2015.06.011
24. Mao K, Zhang W, Yu L, Yu Y, Liu H, Zhang X. Transferrin-decorated protein-lipid hybrid nanoparticle efficiently delivers cisplatin and docetaxel for targeted lung cancer treatment. *Drug Des Devel Ther*. 2021;15:3475–3486. doi:10.2147/DDDT.S296253
25. El-Lakany SA, Elzoghby AO, Elgindy NA, Hamdy DA. HPLC methods for quantitation of exemestane–luteolin and exemestane–resveratrol mixtures in nanoformulations. *J Chromatogr Sci*. 2016;54(8):1282–1289. doi:10.1093/chromsci/bmw063
26. Yue Y, Eun JS, Lee MK, Seo SY. Synthesis and characterization of G5 PAMAM dendrimer containing daunorubicin for targeting cancer cells. *Arch Pharm Res*. 2012;35(2):343–349. doi:10.1007/s12272-012-0215-7
27. Wu R, Zhang Z, Wang B, et al. Combination chemotherapy of lung cancer - co-delivery of docetaxel prodrug and cisplatin using aptamer-decorated lipid-polymer hybrid nanoparticles. *Drug Des Devel Ther*. 2020;14:2249–2261. doi:10.2147/DDDT.S246574
28. Wu C, Xu Q, Chen X, Liu J. Delivery luteolin with folacin-modified nanoparticle for glioma therapy. *Int J Nanomedicine*. 2019;14:7515–7531. doi:10.2147/IJN.S214585
29. Fan X, Wang T, Ji Z, Li Q, Shen H, Wang J. Synergistic combination therapy of lung cancer using lipid-layered cisplatin and oridonin co-encapsulated nanoparticles. *Biomed Pharmacother*. 2021;141:111830. doi:10.1016/j.biopha.2021.111830
30. Haghighi FH, Binaymotlagh R, Mirahmadi-Zare SZ, Hadadzadeh H. Aptamer/magnetic nanoparticles decorated with fluorescent gold nanoclusters for selective detection and collection of human promyelocytic leukemia (HL-60) cells from a mixture. *Nanotechnology*. 2020;31(2):025605. doi:10.1088/1361-6528/ab484a
31. Chou TC. Drug combination studies and their synergy quantification using the Chou-Talalay method. *Cancer Res*. 2010;70(2):440–446. doi:10.1158/0008-5472.CAN-09-1947
32. Truebenbach I, Kern S, Loy DM, et al. Combination chemotherapy of L1210 tumors in mice with pretubulysin and methotrexate lipo-oligomer nanoparticles. *Mol Pharm*. 2019;16(6):2405–2417. doi:10.1021/acs.molpharmaceut.9b00038
33. Bao H, Zheng N, Li Z, Zhi Y. Synergistic effect of tangeretin and atorvastatin for colon cancer combination therapy: targeted delivery of these dual drugs using RGD peptide decorated nanocarriers. *Drug Des Devel Ther*. 2020;14:3057–3068. doi:10.2147/DDDT.S256636
34. Harris TJ, Green JJ, Fung PW, Langer R, Anderson DG, Bhatia SN. Tissue-specific gene delivery via nanoparticle coating. *Biomaterials*. 2010;31(5):998–1006. doi:10.1016/j.biomaterials.2009.10.012
35. Chen Y, Xu Z, Lu T, Luo J, Xue H. Prostate-specific membrane antigen targeted, glutathione-sensitive nanoparticles loaded with docetaxel and enzalutamide for the delivery to prostate cancer. *Drug Deliv*. 2022;29(1):2705–2712. doi:10.1080/10717544.2022.2110998
36. Jing F, Li J, Liu D, Wang C, Sui Z. Dual ligands modified double targeted nano-system for liver targeted gene delivery. *Pharm Biol*. 2013;51(5):643–649. doi:10.3109/13880209.2012.761245
37. Choueiri RM, Klinkova A, Pearce S, Manners I, Kumacheva E. Self-assembly and surface patterning of polyferrocenylsilane-functionalized gold nanoparticles. *Macromol Rapid Commun*. 2018;39(3). doi:10.1002/marc.201700554

38. Yang Z, Li P, Chen Y, et al. Construction of pH/glutathione responsive chitosan nanoparticles by a self-assembly/self-crosslinking method for photodynamic therapy. *Int J Biol Macromol*. 2021;167:46–58. doi:10.1016/j.ijbiomac.2020.11.141
39. Dong Z, Wang Y, Guo J, et al. Prostate cancer therapy using docetaxel and formononetin combination: hyaluronic acid and epidermal growth factor receptor targeted peptide dual ligands modified binary nanoparticles to facilitate the in vivo anti-tumor activity. *Drug Des Devel Ther*. 2022;16:2683–2693. doi:10.2147/DDDT.S366622
40. Zhang R, Ru Y, Gao Y, Li J, Mao S. Layer-by-layer nanoparticles co-loading gemcitabine and platinum (IV) prodrugs for synergistic combination therapy of lung cancer. *Drug Des Devel Ther*. 2017;11:2631–2642. doi:10.2147/DDDT.S143047
41. Pang J, Xing H, Sun Y, Feng S, Wang S. Non-small cell lung cancer combination therapy: hyaluronic acid modified, epidermal growth factor receptor targeted, pH sensitive lipid-polymer hybrid nanoparticles for the delivery of erlotinib plus bevacizumab. *Biomed Pharmacother*. 2020;125:109861. doi:10.1016/j.biopha.2020.109861
42. Wang H, Sun G, Zhang Z, Ou Y. Transcription activator, hyaluronic acid and tocopheryl succinate multi-functionalized novel lipid carriers encapsulating etoposide for lymphoma therapy. *Biomed Pharmacother*. 2017;91:241–250. doi:10.1016/j.biopha.2017.04.104
43. Li S, Wang L, Li N, Liu Y, Su H. Combination lung cancer chemotherapy: design of a pH-sensitive transferrin-PEG-Hz-lipid conjugate for the co-delivery of docetaxel and baicalin. *Biomed Pharmacother*. 2017;95:548–555. doi:10.1016/j.biopha.2017.08.090
44. Chou TC. Theoretical basis, experimental design, and computerized simulation of synergism and antagonism in drug combination studies. *Pharmacol Rev*. 2006;58(3):621–681. doi:10.1124/pr.58.3.10
45. Wang B, Hu W, Yan H, et al. Lung cancer chemotherapy using nanoparticles: enhanced target ability of redox-responsive and pH-sensitive cisplatin prodrug and paclitaxel. *Biomed Pharmacother*. 2021;136:111249. doi:10.1016/j.biopha.2021.111249
46. Jedrzejczyk M, Wisniewska K, Kania KD, Marczak A, Szwed M. Transferrin-bound doxorubicin enhances apoptosis and DNA damage through the generation of pro-inflammatory responses in human leukemia cells. *Int J Mol Sci*. 2020;21(24):9390. doi:10.3390/ijms21249390
47. Choi J, Ko E, Chung HK, et al. Nanoparticulated docetaxel exerts enhanced anticancer efficacy and overcomes existing limitations of traditional drugs. *Int J Nanomedicine*. 2015;10:6121–6132. doi:10.2147/IJN.S88375
48. Li C, Ge X, Wang L. Construction and comparison of different nanocarriers for co-delivery of cisplatin and curcumin: a synergistic combination nanotherapy for cervical cancer. *Biomed Pharmacother*. 2017;86:628–636. doi:10.1016/j.biopha.2016.12.042
49. Zhu B, Zhang H, Yu L. Novel transferrin modified and doxorubicin loaded pluronic 85/lipid-polymeric nanoparticles for the treatment of leukemia: in vitro and in vivo therapeutic effect evaluation. *Biomed Pharmacother*. 2017;86:547–554. doi:10.1016/j.biopha.2016.11.121
50. He F, Wen N, Xiao D, et al. Aptamer-based targeted drug delivery systems: current potential and challenges. *Curr Med Chem*. 2020;27(13):2189–2219. doi:10.2174/0929867325666181008142831
51. Wang L, Wang W, Rui Z, Zhou D. The effective combination therapy against human osteosarcoma: doxorubicin plus curcumin co-encapsulated lipid-coated polymeric nanoparticulate drug delivery system. *Drug Deliv*. 2016;23(9):3200–3208. doi:10.3109/10717544.2016.1162875
52. Liu B, Han L, Liu J, Han S, Chen Z, Jiang L. Co-delivery of paclitaxel and TOS-cisplatin via TAT-targeted solid lipid nanoparticles with synergistic antitumor activity against cervical cancer. *Int J Nanomedicine*. 2017;12:955–968. doi:10.2147/IJN.S115136